Microcellular microspheres and microballoons by precipitation with a vapour–liquid compressed fluid antisolvent

David J. Dixon*, Gabriel Luna-Bárcenas and Keith P. Johnston†
Department of Chemical Engineering, University of Texas, Austin, TX 78712, USA
(Received 9 November 1993; revised 6 February 1994)

A new type of precipitation with a compressed fluid antisolvent (PCA) is demonstrated for the formation of porous polymeric microspheres and microballoons (hollow microspheres). The antisolvent is composed of pure saturated vapour over saturated liquid CO_2. A polystyrene (PS) in toluene solution is sprayed through a capillary into CO_2 vapour to form droplets, which fall into liquid CO_2 where they are rapidly dried and vitrified. Both the thickness and porosity of the microcellular shells can be controlled by changing the initial solution composition. The thickness is inversely proportional to the initial PS concentration. As the concentration is increased there is a transition from porous microballoons to porous microspheres. The cell sizes and surface areas of the microspheres are approximately 1–20 μm and 3–40 $m^2 g^{-1}$, respectively. The mass transfer pathway may be altered by addition of CO_2 to the polymer solution before spraying, resulting in greater and more uniform porosity. Compared with methanol as an antisolvent, CO_2 produces more porous and spherical microspheres, with 7–14 times faster precipitation.

(Keywords: phase separation; polymeric materials; supercritical fluid)

INTRODUCTION

Microstructural polymeric materials, with features of the order of 1–20 μm, can be produced by physical phase separation techniques including thermally induced phase separation (TIPS)[1–3], precipitation with a liquid antisolvent[4–6], spray drying[7], compositional quenching[8], and rapid expansion from supercritical solution (RESS)[9–11] or by chemical reaction[12,13]. Examples of these materials include microspheres, microporous fibres, hollow microporous fibres, asymmetric membranes, highly oriented fibrils ($<1\,\mu$m) and microcellular foams[14,15]. The importance of these materials is evident in the wide variety of practical applications including high-strength-to-weight ratio foams, transparent insulators ($<0.05\,\mu$m pores), doped transparent foams for lasers, artificial skin and blood vessels, controlled-release media, high-strength fibrils, high surface area adsorbents, chromatographic supports, ion-exchange resins, gels, filters, catalyst substrates and porous electrodes[16].

A few years ago microparticles were formed with a new process in which a compressed fluid such as CO_2 is used as an antisolvent, so-called precipitation with a compressed fluid antisolvent (PCA)[17]. Here, a solution is sprayed across a small capillary tube or orifice into a vessel containing a compressed gas, liquid or supercritical fluid which is miscible with the solvent, but immiscible with the solute. According to the polymer literature, the fluid is called a non-solvent. However, we will call it an antisolvent, as has been done in a large number of papers in the supercritical fluid literature. The high diffusion rates and intense atomization can lead to rapid phase separation producing submicrometre particles. Compared with spray drying, the temperature can be much lower and the atomization is more intense, often leading to smaller particles.

The PCA process has been used to form submicrometre microspheres of polystyrene, by spraying low concentrations (<3.5 wt%) of PS in toluene solutions into liquid CO_2 at room temperature[17,18]. Biologically active insulin particles of the order of 4 μm have been formed by spraying dimethylsulfoxide solutions into supercritical CO_2[19]. Submicrometre biodegradable L-poly(lactic acid) particles have been formed by spraying methylene chloride solutions into gaseous, liquid and supercritical CO_2[20,21]. Based on the scanning electron microscopy micrographs in these studies, the particles did not appear to be porous; however, this observation does not preclude the possibility of extremely small pores ($<100\,\mu$m).

A variety of additional types of polymer morphologies may be produced with the PCA process by adjusting the solution concentration and the properties of CO_2 from gaseous to supercritical to liquid conditions. These changes in solvent properties strongly influence binodal and spinodal curves in the phase diagram, interfacial properties, the jet characteristics, transport rates and sorption of CO_2 in the solute. Furthermore, the glass transition temperature of the polymer varies strongly as a function of the CO_2 sorption[22,23].

In addition to nucleating a polymer discrete phase, the PCA process may also be used to nucleate solvent voids

* Present address: Department of Chemistry and Chemical Engineering, South Dakota School of Mines and Technology, Rapid City, SD 57701, USA
† To whom correspondence should be addressed

0032-3861/94/18/3998–08

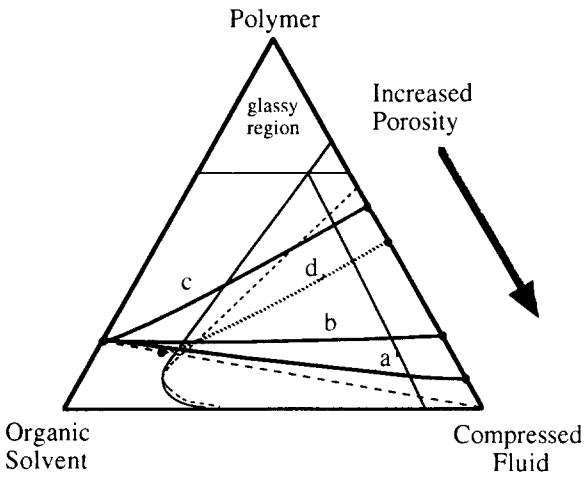

Figure 1 Schematic ternary diagram comparing mass transfer pathways for precipitation with a compressed fluid antisolvent. (——) Binodal curve; (– – – –) spinodal curve[24]

in a polymer continuous phase to produce fibres. Here the initial concentration is sufficiently high that the solution enters the two-phase region on the polymer-rich side of the critical composition (*Figure 1*). Microcellular fibres, some of which were hollow, were produced by increasing the concentration of the sprayed polystyrene solutions above 6%[17,18,24]. Near the critical composition, fibres composed of highly oriented microfibrils are produced at high shear rates, perhaps due to spinodal phase separation and orientation in the discharge jet. More recently, highly oriented fibrils have been produced from very dilute solutions of crystalline polymers[25,26].

The objective of this work is to produce additional morphologies with the PCA process, specifically microcellular microspheres and microballoons (hollow microspheres). A new approach is required since all of the polymer continuous materials made previously (in dense liquid or supercritical CO_2) were fibres. It was proposed that the rapid formation of a skin on the surface of the jet prevents atomization, such that fibres are produced. The skin formation is due to rapid inward diffusion of CO_2 and outward diffusion of toluene. If a polymer solution were sprayed into a CO_2 environment in which toluene is not very soluble, such as vapour CO_2, skin formation may be delayed and the jet may break up into discrete droplets. However, this technique was found to produce agglomerated polymer, since the droplets do not dry fast enough[18].

To attempt to prevent fibre formation, we have chosen to spray a polymer solution into a two-phase mixture of pure vapour and liquid CO_2 at the saturation temperature[17]. Our hypothesis is that the jet will have sufficient time to break up in the vapour phase into droplets, which then fall into the liquid phase, where they are rapidly dried and hardened. To control the morphologies of the microcellular microspheres and microballoons, the mass transfer pathways and solution viscosity have been varied. The Results section begins by considering the effects of the concentration of the polymer solution and the flow rate of the jet on the morphology. In the next section, CO_2 is added to the feed to move the starting solution closer to the two-phase region and to lower the viscosity. These results are then compared with conventional experiments in which liquid methanol is used as an antisolvent. The different diffusion coefficients in these systems should result in distinctly different mass transfer paths, precipitation times, and thus final polymer morphologies.

EXPERIMENTAL

Polystyrene (PS) (Pressure Chemicals, $M_w = 200\,000$, $M_w/M_n = 1.05$, or Scientific Polymer Products, $M_w = 280\,000$, $M_w/M_n = 2.37$) and toluene (Fischer, ACS grade) were used as received. Solutions of PS in toluene were sprayed through a 151 μm internal diameter (i.d.) by 18 cm long fused silica capillary tube. A 2.54 cm outer diameter (o.d.) × 1.746 cm i.d. × 20.3 cm long stainless steel vertical spray vessel (Autoclave Engineers), described in detail previously[24], was used for most of the vapour over liquid experiments. The experimental setup for the vertical spray vessel is shown schematically in *Figure 2* with a CO_2 interface present. The interface level was chosen near the middle of the vessel to allow ample distance for the liquid polymer solution jet to break up, while maintaining sufficient liquid CO_2 to solidify the polymer microspheres. A known volume of CO_2 was added to the vessel. By knowing the system temperature, volume and pressure the location of the interface was determined.

The spray vessel, which contained the CO_2, was allowed to equilibrate at 22°C before the polymer solution was sprayed. CO_2 was not added while spraying and the solution was typically sprayed for 10–20 s. After spraying, CO_2 was added to fill the cell with liquid at 70 bar (7×10^6 Pa) and 22°C. The bottom vent valve was opened and CO_2 was swept through the cell to remove the solvent fully while the pressure was maintained at a constant value. After approximately 50 min purging, the system was slowly depressurized over a 30 min period.

The resulting microspheres were prepared for observation by a scanning electron microscope (s.e.m.) by freezing

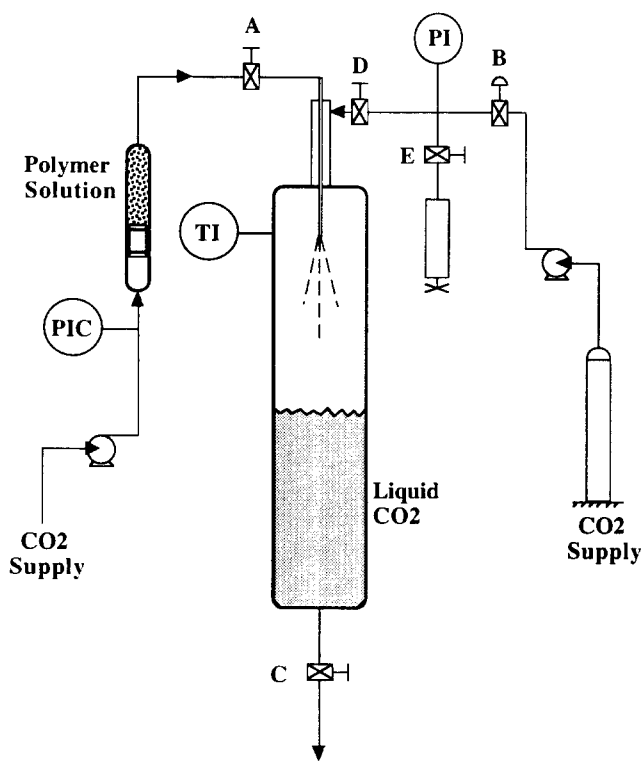

Figure 2 Apparatus for spraying a polymer solution into CO_2 vapour over a pool of liquid CO_2, leading to formation of polymer microspheres and microballoons

them directly in liquid nitrogen, and immediately cutting them in half. The samples were mounted on a piece of double-sided sticky carbon tape, attached to a 3/8 in × 3/8 in (0.94 cm × 0.94 cm) brass s.e.m. cylinder, sputter coated with gold–palladium, and imaged in the s.e.m. (Jeol JSM-35C).

Addition of CO_2 antisolvent to the solution of PS in toluene prior to spraying has been described in detail previously[18,24]. The solutions with pre-added antisolvent were still one-phase, as verified by separate phase equilibrium experiments[17].

RESULTS AND DISCUSSION

Microspheres by vapour over liquid PCA

In this set of experiments, the concentration of PS was varied from 6 to 25.8% by weight. These concentrations were chosen such that the mass transfer pathways cross the polymer-rich side of the two-phase region (see *Figure 1*). As the polymer concentration increases, the mass transfer pathways move towards decreased porosity.

A 6 wt% solution of PS in toluene was sprayed into the vertical cell, which contained approximately equal amounts of liquid and vapour CO_2 at its vapour pressure. Hollow microspheres or microballoons were formed as shown in *Figure 3*. The wall or shell of these microballoons was quite thin ($\sim 20\,\mu m$) and contained 1–10 μm pores. Based on this morphology, it is highly likely that the polymer solution jet broke up in the vapour phase of CO_2 to form discrete droplets. This assumption was later confirmed by observation of the jet breakup in a clear high-pressure sapphire tube described previously[17]. This result is remarkable because a 6% PS solution that was sprayed into liquid CO_2 at the same temperature resulted in fibres[24]. Although the microballoons are fairly spherical, some distortion occurred, probably before the initially formed thin shell grew and hardened.

The microsphere is larger than the capillary diameter. This growth could have been caused in part by swelling due to CO_2 dissolution, by Rayleigh instabilities and by coalescence of droplets.

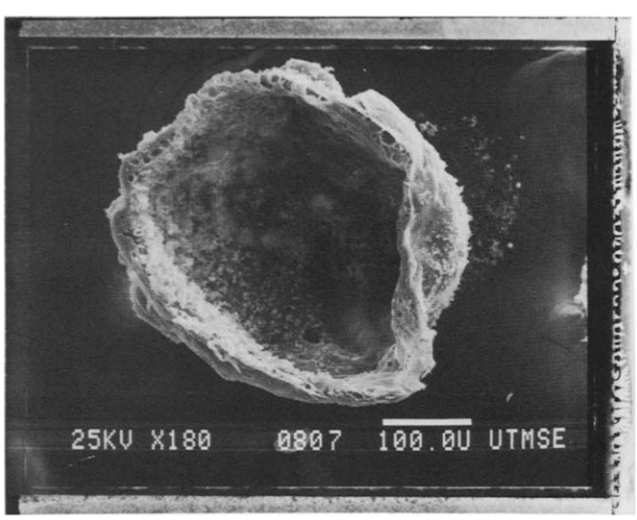

Figure 3 S.e.m. photograph of a polystyrene microsphere formed by spraying a 6% solution of polystyrene in toluene through a 151 μm nozzle into CO_2 vapour over a pool of CO_2 liquid under the following conditions: $T = 22°C$, vapour density = 0.211 g cm^{-3}, $P = 60$ bar and ΔP across the nozzle = 69 bar (1 bar = 1×10^5 Pa)

To explore the mechanism of microballoon formation in greater detail, a semiquantitative estimation of the half-time ($t_{1/2}$), to reach half the saturation value for CO_2 in the droplet was made. A droplet diameter of 330 μm (same as in *Figure 3*) was assumed. An approximate form of the short-time solution for diffusion in a sphere is[27]:

$$\frac{M_t}{M_\infty} = \frac{6}{a}\sqrt{\frac{Dt}{\pi}} \tag{1}$$

where M_t is the mass transferred at time t, M_∞ is the saturation value, a is the sphere radius and D is the diffusion coefficient. For $M_t/M_\infty = 0.5$, equation (1) can be rewritten as:

$$t_{1/2} = 0.0218a^2/D \tag{2}$$

Assuming the CO_2 diffuses through toluene, the diffusivity is of the order of 10^{-5} cm^2 s^{-1} and $t_{1/2} \approx 0.6$ s. The jet velocity is estimated as 96 cm s^{-1}, and the time to fall through the vapour phase is ~ 0.1 s. Thus phase separation can begin while still in the vapour phase.

Pinnau[4], Strathmann and Kock[28] and others have suggested that a dense skin can form rapidly in polymer membrane formation using a liquid antisolvent. The same is true for fibre formation by PCA with CO_2 as the antisolvent[24]. In the present study, the $t_{1/2}$ for CO_2 to diffuse into the outer 2 μm of the droplet is of the order of 10^{-4} s. Thus it is likely that skin formation already begins to develop in the vapour phase. Once this sphere contacts the liquid CO_2 phase, any toluene on the surface will transfer rapidly into the liquid CO_2, since the two liquids are miscible. Consequently, the outer shell is hardened, in a similar manner to fibre formation in liquid CO_2.

We now present a mechanism to explain the formation of the hollow cores. Suppose a skin forms on a drop with a diameter of the same order as that of the capillary tube. Then for a polymer weight fraction x, the porosity is approximately $1-x$, since the densities of polymer and solvent are similar. The pores could be distributed all the way to the centre or a hollow core could be present. As the polymer concentration is decreased, it becomes less likely that the walls about the pores would remain thick enough to persist all the way to the centre of the sphere.

The skin vitrifies quickly since the temperature is below the T_g for polystyrene containing dissolved CO_2[22,23]. Consequently, little time is available for growth of solvent voids, which remain very small. The diffusion coefficient of CO_2 through this glassy skin exceeds that of toluene[24]. Therefore, CO_2 will enter the core faster than toluene leaves it, so that the polymer concentration will decrease in the core. The solvent-rich droplets will have much more time to grow and coalesce, because the toluene concentration in the core will be sufficient to prevent vitrification of the polymer. This mechanism explains the increase in the size of the pores from the outer surface of the shells to the inner surface. Also, since the polymer concentration is reduced by the addition of CO_2, the precipitated polymer phase will be more dilute (see curve a in *Figure 1*). As the solvent-rich droplets grow and coalesce, the thin dilute polymer-rich channels about these droplets will rupture, causing the polymer to collapse against the inner surface of the shell of the microballoon. The polymer concentration may become sufficiently dilute that a polymer continuous phase may no longer form upon phase separation in the core. The

above mechanism is supported by the trends in the morphologies of the microballoons and microspheres throughout this study. It is analogous to the mechanism for the formation of hollow and solid porous fibres described previously[24].

If it is assumed that the microsphere in *Figure 3* was formed from a droplet of liquid polymer solution of the same size, and further that all the toluene is removed leaving only the original amount of PS, then the expected shell thickness may be estimated. First, if it is assumed the polymer precipitates into a non-porous shell at the normal density of polystyrene ($1.05\,g\,cm^{-3}$), then the expected thickness would be $\sim 3\,\mu m$. Since pores are visible and the actual thickness is estimated to be $\sim 20\,\mu m$, the shell porosity is estimated as $\sim 84\%$. Unfortunately, the amount of sample collected was too small to do BET or Hg porosimetry measurements of pore volume. High-speed photography could be used to determine the actual size of the drops in the spray; however, there are some difficulties, such as obtaining high magnification at the large working distances required by the size of the existing high-pressure vessel.

It is possible that the morphology could be altered during depressurization if the polymer is in the rubbery state[14,15,17]. The T_g of PS in the presence of CO_2 has been predicted theoretically[22] and measured experimentally[23] in terms of the creep compliance. At 70 bar (7×10^6 Pa), the T_g is 35°C, so the microspheres should have been glassy during depressurization.

In order to determine if the radius of the hollow core of the microsphere is a function of polymer concentration, experiments were done at higher initial polymer solution compositions. For a 10% PS solution, *Figure 4* shows that hollow microspheres again are formed, but now the wall thickness has increased. Here the walls are 30–50 μm thick with 1–10 μm pores. The particles are more spherical. The increase in the shell thickness and the more spherical shape are due to the increased concentration and the higher solution viscosity. The higher solution viscosity would act to stabilize the precipitated shell by limiting the effects of deformation forces, a trend that becomes more obvious as the initial polymer solution concentration is further increased.

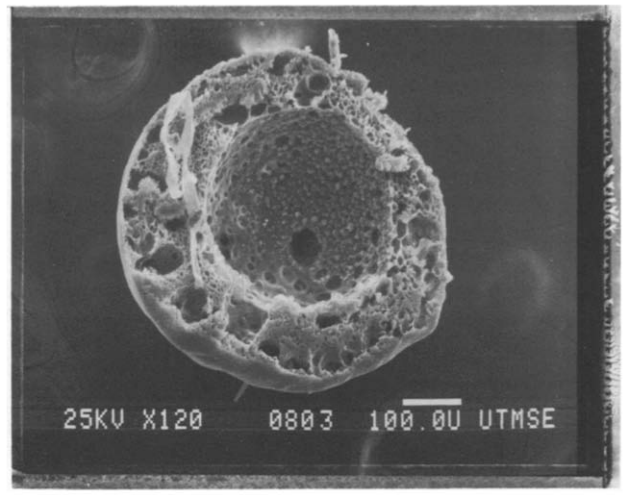

Figure 5 S.e.m. photograph of a polystyrene microsphere formed by spraying a 12.8% solution of polystyrene in toluene under conditions the same as in *Figure 3*

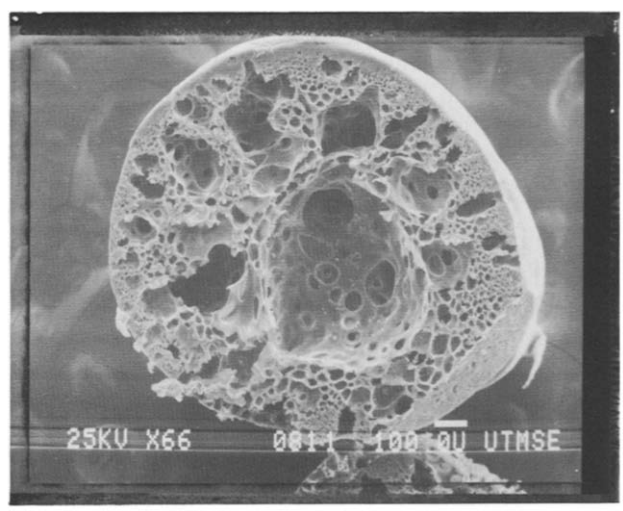

Figure 6 S.e.m. photograph of a polystyrene microsphere formed by spraying a 16% solution of polystyrene in toluene under conditions the same as in *Figure 3*, except that ΔP across the nozzle = 103.4 bar (1 bar = 1×10^5 Pa)

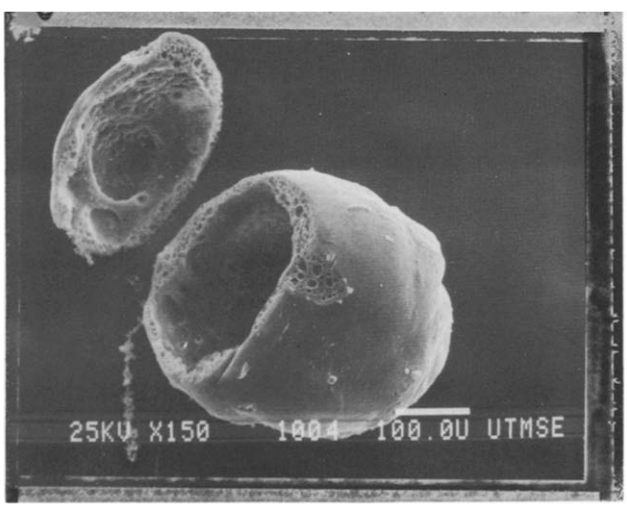

Figure 4 S.e.m. photograph of a polystyrene microsphere formed by spraying a 10% solution of polystyrene in toluene under conditions the same as in *Figure 3*

Increasing the PS concentration to 12.8 wt%, while keeping the pressure drop (ΔP) across the capillary, the temperature and the CO_2 conditions constant, results in microspheres with a shell ~ 120–$150\,\mu m$ thick (*Figure 5*). The shell is porous and while it contains many 1–10 μm pores, there are also some larger macrovoids that are 50–100 μm in diameter. Macrovoids have also been observed in liquid antisolvent-induced phase separation[4]. Some of the macrovoids appear to emanate from the surface region. These surface region macrovoids may form because a small hole or defect in the skin developed, allowing a bubble of CO_2 to form and grow before the surface hole 'healed' and the system solidified. This mechanism does not explain the appearance of interior macrovoids. It is likely that the internal macrovoids form due to growth and/or coalescence of solvent-rich pockets in the 'wet' interior.

If it is again assumed that the original droplet is the same size as the final microsphere in *Figure 5* ($\sim 500\,\mu m$),

then it is estimated that the solid shell thickness would be $\sim 10\,\mu m$. Because the actual shell is much thicker, the porosity of the shell is estimated to be 88%, with an apparent shell density of $0.128\,g\,cm^{-3}$. Since it is not obvious that this $500\,\mu m$ sphere came from a droplet of the same size, the porosity is somewhat in error. To place a bound on this error, if one assumes that the initial droplet is actually 20% larger ($600\,\mu m$ diameter), then the observed shell porosity would be approximately 10% lower. Finally it is estimated the surface area could range from $3–40\,m^2\,g^{-1}$, depending on the average size of the pores.

For a further increase in the initial PS concentration to 16% (*Figure 6*) the trend of decreasing radius of the hollow core continues. The morphology is interesting because the void structure is asymmetric and it contains a large number of macrovoids. By closely examining the macrovoids, small pores or openings can be seen in the walls between the cells. The pores indicate that the walls were in the process of rupturing when the system morphology was vitrified. The rupturing of the smaller cell walls explains, in part, how the macrovoids are formed and grow within the interior of the microsphere. It is reasonable to assume the interior of the sphere stays 'wet' with toluene longer than the exterior so that when phase nucleation occurs the interior has a longer time for growth, while the outer region is precipitated and vitrified sooner, thus preserving the small cell sizes. The outer surface of the microsphere is a continuous dense skin. This skin appears defect-free, as observed within the resolution of the s.e.m. (down to $\sim 0.1\,\mu m$).

At a 20% PS concentration (*Figure 7*) the microspheres are no longer hollow, but fully porous, with a continuous pore structure inside. A similar asymmetric structure is observed as in *Figure 6*. Here, however, the macrovoids appear to radiate from the surface. The apparent lack of internal macrovoids may be due to the relative sizes of the microspheres shown and to the higher concentration. For comparison, the microspheres shown in *Figure 8* were also formed from a 20% PS solution, but at a lower velocity. They contain internal macrovoids, and their radii are ~25% larger than for those in *Figure 7*. Thus

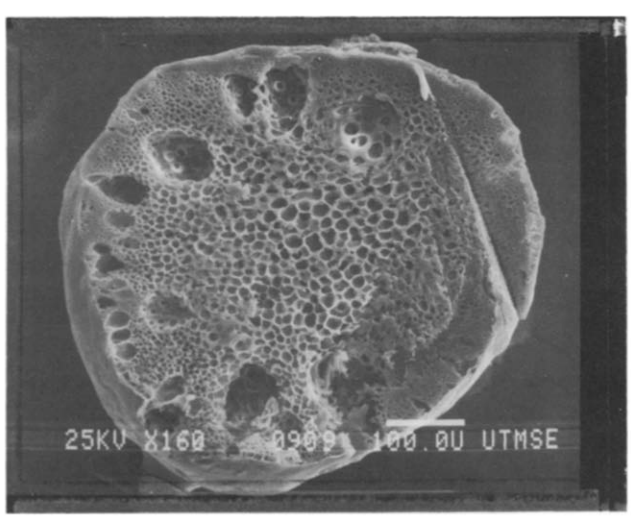

Figure 7 S.e.m. photograph of a polystyrene microsphere formed by spraying a 20% solution of polystyrene in toluene under conditions the same as in *Figure 3*, except that ΔP across the nozzle was 103.4 bar (1 bar = 1×10^5 Pa)

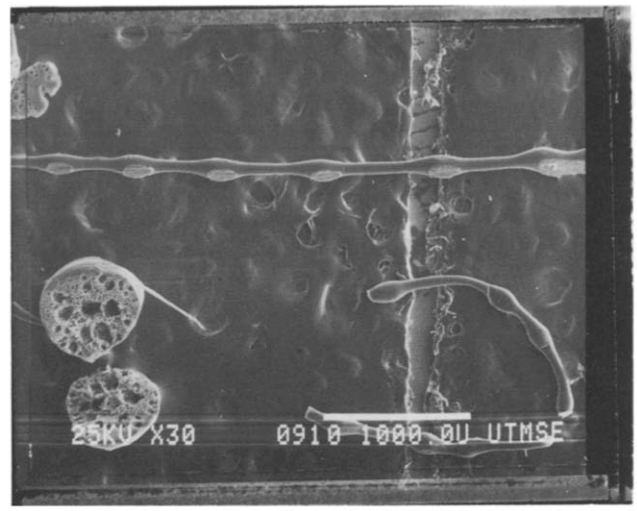

Figure 8 S.e.m. photograph of polystyrene morphology formed by spraying a 20% solution of polystyrene in toluene under conditions the same as in *Figure 3*

it seems reasonable that in cases with longer diffusion times, more growth of voids can occur, resulting in more macrovoids. The estimated porosity and surface area for the 20% experiment in *Figure 7* are virtually the same as for the 12.8% case, and are 84% and $3–30\,m^2\,g^{-1}$, respectively.

An overall trend observed so far is that as the concentration is increased the radius of the hollow core steadily decreases. This supports the trend shown previously with fibres[24]. Also, as outlined in *Figure 1*, the more polymer contained in the feed composition, the lower the final porosity. However, in this work, the size of the core changed more than the size of the pores. If the concentration of the initial polymer solution was increased further, it is suspected that the pore size would begin to decline significantly, once the hollow core is removed.

With the 20% PS solution another transition region was noted. Microspheres and fibres were collected at this concentration and also at an even higher initial PS concentration of 25.8%. *Figure 8* shows some of the fibres produced for a 20% concentration. These fibres show oscillations which are a precursor to jet breakup. For low flow velocities and low viscosity solutions, Levich[29] predicts the breakup wavelength is approximately nine times the radius of the jet. For jets with a high viscosity the breakup wavelength is a somewhat more complex function[29]:

$$\lambda \sim 13\left(\frac{\nu^2 \rho a^3}{\sigma}\right)^{1/4} \tag{3}$$

where λ is the wavelength, ν is the kinematic viscosity, ρ is the solution density, a is the jet radius and σ is the interfacial tension. Estimating the viscosity of a 20% solution jet as the measured viscosity[24], then $\lambda \sim 0.422/(\sigma^{0.25})$ cm. Assuming a low interfacial tension of 2 dynes cm^{-1}, which may be a lower bound, $\lambda \sim 47a$. An interfacial tension of 30 dynes cm^{-1} (toluene in air is 28 dynes cm^{-1}) results in $\lambda \sim 24a$. This is closer to the value of $18a$, estimated from *Figure 8*. Equation (3) is an approximation for jets with high viscosities, but it does not consider any viscoelastic effects. Nevertheless, it may prove of some value for predicting jet breakup lengths in PCA for vapour over

liquid sprays, especially if more accurate interfacial tensions become available.

At the elevated polymer concentrations of 20 and 25.8% PS, many fibres were collected with few microspheres. To determine why this occurred, observations were made of the jet behaviour by spraying a 25.8% solution into a clear sapphire tube. When the solution was sprayed into air with a ΔP of 56 bar (5.6×10^6 Pa), the flow was dropwise and no jet development was observed. When the same solution at the same ΔP was sprayed into vapour over liquid CO_2, the flow was not dropwise but rather formed a very fine thread that hardened rapidly in the CO_2 liquid phase. The approximate falling distance through the vapour phase was ~ 5 cm. By analysis of the jet breakup, for example by equation (3), it can be seen that changing the solution viscosity or interfacial tension will affect the breakup length of the jet. Increasing the viscosity will stabilize the jet, leading to longer jet lengths before breakup, while increasing interfacial tension has the opposite effect. In the above example, with dropwise flow forming in air, it is probable that the moderate liquid solution viscosity combined with a relatively large interfacial tension (~ 30 dynes cm^{-1}), opposed the formation of a jet. In the experiment with vapour over liquid CO_2, the interfacial tension between the polymer solution and CO_2 vapour is initially much lower than between the solution and air. Also, the rapid mass transfer of CO_2 into the jet causes surface precipitation that increases the surface viscosity. This combination of effects stabilizes the jet leading to fibres. At initial PS concentrations lower than 20%, the jet can break up due to the lower initial solution viscosity and longer time for surface precipitation. Theory has not been developed sufficiently to consider the viscoelastic effects in a highly compressible fluid, which may play an important role at these concentrations.

Antisolvent addition prior to spraying

Figure 1 shows that adding antisolvent to the starting solution will shift the final polymer composition away from the polymer vertex producing a more porous microsphere. *Figure 9* is a hollow microsphere formed by spraying a 10.8% PS (in PS–toluene–CO_2) solution,

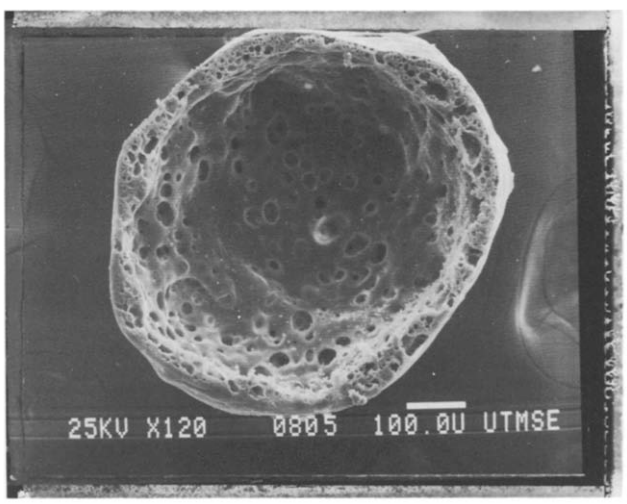

Figure 9 S.e.m. photograph of a polystyrene microsphere formed by spraying a 10.85% solution of polystyrene in toluene with pre-added CO_2 (15.2 wt% CO_2 added to a 12.8% polystyrene solution), under conditions the same as in *Figure 3*

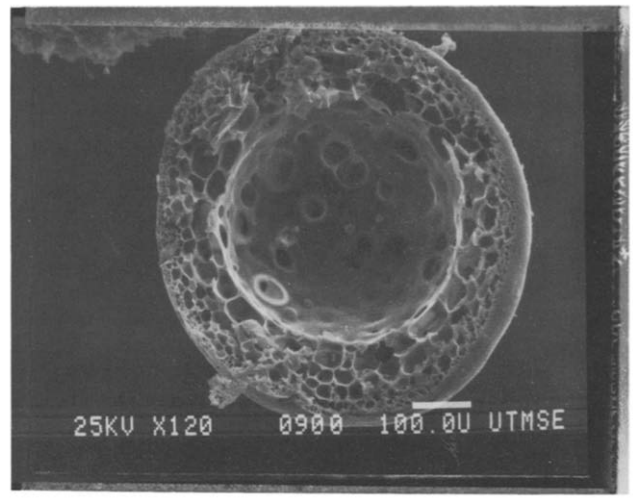

Figure 10 S.e.m. photograph of a polystyrene microsphere formed by spraying a 12.2% solution of polystyrene in toluene with pre-added CO_2 (23.6 wt% CO_2 added to a 16% polystyrene solution), for conditions the same as in *Figure 3*, except that ΔP across the nozzle = 103.4 bar (1 bar = 1×10^5 Pa)

containing dissolved CO_2, into the vapour phase of CO_2 over a liquid CO_2 pool. The shell of the hollow microsphere contains pores from 1–30 μm and is ~ 50 μm thick. This morphology is nearly identical to *Figure 4*, where the initial polymer in toluene solution concentration was 10% and did not contain any predissolved CO_2. It appears in this instance that CO_2 acts as a diluent.

Increasing the polymer concentration to 12.2% PS (in PS–toluene–CO_2 solution) results in microspheres that are less hollow, consistent with the results obtained above, and previously with fibres[17,24]. *Figure 10* is an example of one of these microspheres showing that the thickness of the shell is comparable to *Figure 5*, in which the PS concentration was 12.8% and no CO_2 was pre-added. A distinct difference between the two experiments is evident in the cell structure. With pre-added CO_2 the cells appear to be more uniform with no macrovoids present. It is proposed that this is due primarily to the time for growth and rupture of the cells. In the experiment with CO_2 pre-added, only ~ 10 wt% more CO_2 must be transferred into the microsphere to cause phase separation. Thus, there will be less time for growth of solvent–antisolvent cells and also for walls between the cells to rupture. Likewise, less time will be required to reach a composition where the morphology is vitrified. In contrast, the experiment with no pre-added CO_2 requires that $\sim 34\%$ CO_2 must be transferred into the microsphere for phase separation, thus allowing more time for growth in the interior of the sphere.

Methanol as an antisolvent

In order to place the above results in perspective, conventional experiments have been performed by spraying solutions of PS in toluene into methanol at ambient pressure. Methanol is a common antisolvent for PS and is miscible with the low concentrations of toluene experienced during the experiments. *Table 1* shows the results for a 16% PS solution sprayed into either methanol or CO_2 at 22.5°C. In the former case, the methanol was stirred in a 250 ml beaker. For the experiments with CO_2, the solution was sprayed into the vapour phase and allowed to fall ~ 5 cm into a pool of liquid CO_2 (without stirring).

Table 1 Comparison of time for microspheres to turn opaque in methanol or a mixture of vapour and liquid CO_2 at 22°C when formed from a 16 wt% solution of polystyrene in toluene

Antisolvent	Particle size (μm)	ΔP (bar) across nozzle	Macrostructure	Time to opacity (s)	Stirring
MeOH	~1400	104	Wafers	349	No
MeOH	~1200	104	Wafers	180	Yes
MeOH	~500	173	Hollow spherical caps	180	Yes
CO_2	~800	104	Hollow microspheres	25	No
CO_2	~800	70	Hollow microspheres	22	No

1 bar = 1×10^5 Pa

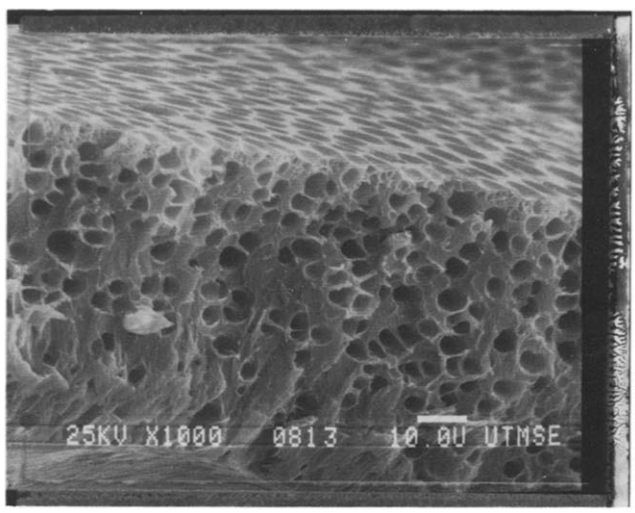

Figure 11 S.e.m. photograph of a section of a polystyrene particle formed by spraying a 16% solution of polystyrene in toluene through a 151 μm nozzle into liquid methanol at 22°C and with a ΔP across the nozzle of 103.4 bar (1 bar = 1×10^5 Pa)

In the first two experiments, the flow was dropwise and the droplets fell through about 5 cm of air before landing in the methanol. The droplets fully collapsed into wafer-like discs that were ~100 μm thick. The time listed in *Table 1* is the time measured for the particle to appear visually fully white and opaque. It was observed prior to this point that the particles appeared 'wet' and would stick to each other if they collided. Gentle stirring in the beaker dramatically decreased the time for the particles to become fully opaque. *Figure 11* is a s.e.m. photograph of the cross-section of one of these discs. The pores are ~1–5 μm in diameter. The cell structure and cell density are comparable to fibres seen previously[24], which were formed by spraying the same solution directly into liquid methanol (without a vapour gap). In the third experiment a higher ΔP was used, forming a 1–1.5 cm long jet that broke up into droplets. The final particles appear as half spheres with the bottom flattened. This suggests that the particles may have been spherical, but still soft, when they landed on the bottom of the beaker. The particles are also hollow with approximately 100 μm thick shells and a pore structure similar to *Figure 11*.

For the experiments that used CO_2 in *Table 1*, the flow was dropwise. It was observed that the particles become opaque about 7–14 times faster than when precipitated by methanol, due to higher diffusion rates. As an example, the half-time ($t_{1/2}$) was estimated for the diffusion of methanol into a slab with a half-thickness of 50 μm. An approximate form of the half-time solution for diffusion in a slab is[27]:

$$t_{1/2} = 0.0492h^2/D \quad (4)$$

where h is the total thickness of the slab. With the diffusivity of methanol in PS estimated as 10^{-9} cm^2 s^{-1}, $t_{1/2} \approx 1200$ s. For the CO_2 experiment, approximating the shell as a slab 200 μm thick, and the diffusivity as 10^{-7} cm^2 s^{-1} (ref. 30), gives a half-time of $\approx$49 s. The value is about 25 times less than that for methanol, which is the same order of magnitude ratio as observed experimentally in *Table 1*. The differences between this estimate and experiment are due to the uncertainty in observing full opacity, and in specifying the diffusion coefficients.

Because it was possible that the methanol-precipitated particles flattened when they landed on the bottom of the beaker in a still 'wet' state, a second set of experiments was done (see *Table 2*). In the first two experiments in *Table 2* solutions were sprayed into a 500 ml graduated cylinder filled with methanol. The distance from the end of the nozzle to the liquid interface was 2.5 cm and 10 cm for the first and second experiments, respectively. In the first experiment the flow was dropwise and as the drops fell through the liquid methanol, they flattened into wafer-like discs. The time-scale until they turned opaque was similar to those observed in *Table 1*. To decrease the size of the droplets, the jet velocity was increased and the results show that the final particle size was smaller. An example of one of the more spherical particles is shown on the right in *Figure 12*. This figure shows a hollow, dimpled sphere that has a relatively dense skin containing a few 1–3 μm pores. However, this sphere was the exception as most of the particles were collapsed and were more like the particle on the left. No attempt was made to optimize the procedure to create more spherical particles in methanol, if possible. Comparing the morphology in *Figure 12* with that in *Figure 5*, which was produced with CO_2, shows a dramatic difference in the shell structure. Again, this is probably due to the significant differences between the diffusion rates of CO_2 and methanol, as discussed previously. *Figure 1* shows schematically how different mass transfer paths will influence the porosity. Thus, the slower transfer of methanol would follow a path similar to curve c resulting in a fairly dense shell as observed. The faster transfer of CO_2 would follow a path similar to curve a and result in a more porous shell.

Table 2 Comparison of particle morphology for a 12.8 wt% solution of polystyrene in toluene sprayed into either methanol or a mixture of vapour and liquid CO_2 at 22°C

Antisolvent	Particle size (μm)	ΔP (bar) across nozzle	Macrostructure	Microstructure
MeOH	~1400	67	Wafers	–
MeOH	~500	208	Collapsed hollow microspheres	Fairly dense with 1–2 μm pores
CO_2	~800	104	Hollow microspheres	Porous with macrovoids

1 bar = 1×10^5 Pa

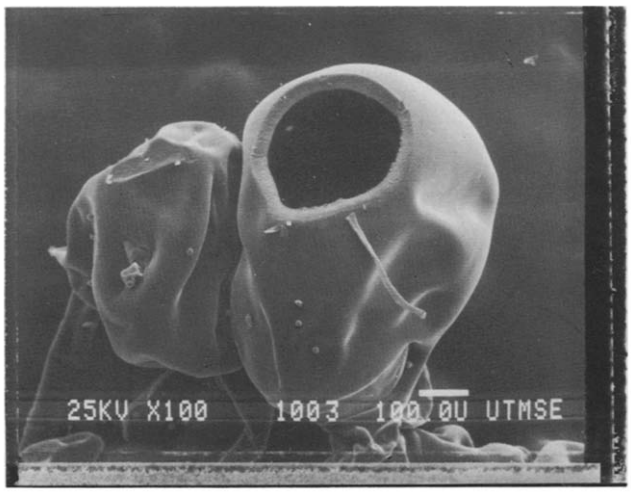

Figure 12 S.e.m. photograph of a polystyrene particle formed by spraying a 12.8% solution of polystyrene in toluene through a 151 μm nozzle into air and allowing the droplets to fall into liquid methanol at 22°C and with a ΔP across the nozzle of 206.8 bar (1 bar = 1×10^5 Pa)

CONCLUSIONS

By spraying 6 to 16 wt% polymer solutions into vapour over liquid CO_2, polymeric microcellular microspheres and microballoons were successfully made. The jet breaks up into droplets in the CO_2 vapour phase, without fibre formation, and the droplets are quenched rapidly in the liquid CO_2 phase. The size of the hollow core of the microballoons is inversely proportional to the initial polymer solution concentration. The formation of the hollow cores may be attributed to growth and coalescence of the solvent–antisolvent voids in the interior region, while it is still wet with toluene. The wet conditions are caused by the rapid influx of CO_2 and the relatively slower loss of toluene from the microspheres. As the solvent-rich voids grow and coalesce, the thin dilute polymer-rich walls about these voids will rupture, causing the polymer to collapse against the inner surface of the shell of the microballoon. This mechanism also explains the increase in the size of the pores from the outer skin of the shells to the inner surface. For PS concentrations greater than or equal to 20%, polymer-rich domains are formed throughout the sphere and a hollow core is not present. Also, both fibres and microspheres are formed due to higher viscosity and skin formation, which stabilize the jet.

The addition of CO_2 to the polymer solution prior to spraying produces two significant effects. First, it acts as a diluent, reducing the polymer concentration and thus increasing the size of the hollow core of the microcellular microsphere. Second, it creates a more uniform pore structure in the shell, probably by decreasing the time for cell growth. The time for growth is reduced since the mass transfer pathway starts closer to the boundary for phase separation. It is likely that a decrease in temperature would also lead to more uniform pores, as the polymer would reach the glassy region sooner.

As observed in previous studies of fibres, CO_2 can be used as an antisolvent to produce very different morphologies than methanol. In many cases, the experiments with methanol led to collapsed PS microspheres with low porosity in the skins. These differences are due primarily to faster diffusion rates of CO_2, which cause precipitation ~7–14 times faster than methanol. The faster diffusion of antisolvent relative to solvent will move the mass transfer pathway downwards, thus increasing the porosity. Lower porosities were also observed for fibres made in methanol *versus* CO_2[24]. In the future, it would be interesting to examine variations in flow rate and nozzle diameter to influence particle size.

ACKNOWLEDGEMENTS

The authors acknowledge the Separations Research Program at the University of Texas at Austin, the State of Texas Energy Research in Applications Program, and the Camille and Henry Dreyfus Foundation for a Teacher-Scholar Grant (to K.P.J.). They are grateful to Don Paul, Bill Koros, Roland Bodmeier, Lisa Wang and Robert Schechter for many helpful discussions.

REFERENCES

1 Aubert, J. H. and Clough, R. L. *Polymer* 1985, **26**, 2047
2 Lloyd, D. R., Kim, S. S. and Kinzer, K. E. *J. Membrane Sci.* 1991, **64**, 1
3 Tsai, F. and Torkelson, J. M. *Macromolecules* 1990, **23**, 775
4 Pinnau, I. *PhD Thesis*, University of Texas at Austin, Austin, TX, 1991
5 Smolders, C. A. 'Proceedings of the Symposium on Ultrafiltration Membranes and Applications', Plenum Press, New York, 1980
6 Kawashima, Y., Niwa, T., Takeuchi, H., Hino, T. and Ito, Y. *J. Controlled Release* 1991, **16**, 279
7 Bodmeier, R. and Chen, H. *J. Pharm. Pharmacol.* 1988, **40**, 754
8 Nauman, E. B., Ariyapadi, M. V., Balsara, N. P., Grocela, T. A., Furno, J. S., Liu, S. H. and Mallikarjun, R. *Chem. Eng. Commun.* 1988, **66**, 29
9 Matson, D. W., Fulton, J. L., Petersen, R. C. and Smith, R. D. *Ind. Eng. Chem. Res.* 1987, **26**, 2298
10 Tom, J. W. and Debenedetti, P. G. *J. Aerosol Sci.* 1991b, **22**, 555
11 Lele, A. K. and Shine, A. D. *AIChE J.* 1992, **38**, 742
12 Pekala, R. W. *J. Mater. Sci.* 1988, **24**, 3221
13 Srinivasan, G. and Elliott, J. R. Jr. *Ind. Eng. Chem. Res.* 1992, **31**, 1414
14 Kumar, V. and Suh, N. P. *ANTEC '88* 1988, 715
15 Goel, S. K. and Beckman, E. *AIChE J.* submitted
16 Aubert, J. H. and Sylwester, A. P. *Chemtech* 1991, **May**, 290
17 Dixon, D. J. *PhD Dissertation*, University of Texas at Austin, Austin, TX, 1992
18 Dixon, D. J. and Johnston, K. P. *AIChE J.* 1993, **39**, 127
19 Yeo, S. D., Lim, G. B., Debenedetti, P. G. and Bernstein, H. *Biotechnol. Bioeng.* 1993, **41**, 341
20 Randolph, T. W., Randolph, A. D., Mebes, M. and Yeung, S. *Biotechnol. Prog.* 1993, **9**, 429
21 Bodmeier, R., Wang, H., Dixon, D. J., Mawson, S. and Johnston, K. P. *Pharmaceut. Res.* submitted
22 Condo, P. D., Sanchez, I. C., Panayiotou, C. G. and Johnston, K. P. *Macromolecules* 1992, **25**, 6119
23 Condo, P. D., Paul, D. R. and Johnston, K. P. *Macromolecules* in press
24 Dixon, D. J. and Johnston, K. P. *J. Appl. Polym. Sci.* 1993, **50**, 1929
25 Yeo, S. D., Debenedetti, P. G., Radosz, M. and Schmidt, H. W. *Macromolecules* 1993, **26**, 6207
26 Luna-Bárcenas, G., Kanakia, S., Sanchez, I. C. and Johnston, K. P. manuscript in preparation
27 Crank, J. 'The Mathematics of Diffusion', Oxford University Press, New York, 1975
28 Strathmann, H. and Kock, K. *Desalination* 1977, **21**, 241
29 Levich, V. J. 'Physicochemical Hydrodynamics', Prentice-Hall, Englewood Cliffs, NJ, 1962
30 Berens, A. R. and Huvard, G. S. *Am. Chem. Soc., Symp. Ser.* 1989, **406**, 207